*Accelerated Publications*

# Abp1p and Fyn SH3 Domains Fold through Similar Low-Populated Intermediate States†

Dmitry M. Korzhnev,[‡,§,#] Philipp Neudecker,[‡,§,#] Arash Zarrine-Afsar,[‡] Alan R. Davidson,[‡,#] and Lewis E. Kay*[,‡,§,#]

*Department of Biochemistry, University of Toronto, Toronto, Ontario, Canada, M5S 1A8, Department of Chemistry, University of Toronto, Toronto, Ontario, Canada, M5S 3H6 and Department of Medical Genetics, University of Toronto, Toronto, Ontario, Canada, M5S 1A8*

*Received June 9, 2006; Revised Manuscript Received July 12, 2006*

ABSTRACT: Src homology 3 (SH3) domains are small modules that are thought to fold via a two-state mechanism, without the accumulation of significant populations of intermediate states. Relaxation dispersion NMR studies of the folding of G48V and G48M mutants of the Fyn SH3 domain have established that, at least for these modules, folding proceeds through the formation of a transient on-pathway intermediate with an equilibrium population of 1−2% that can be readily detected [Korzhnev, D. M., et al. (2004) *Nature 430*, 586−590]. To investigate the generality of this result, we present an $^{15}N$ relaxation dispersion NMR study of a pair of additional SH3 domains, including a G48V mutant of a stabilized Abp1p SH3 domain that shares 36% sequence identity with the Fyn SH3 module, and a A39V/N53P/V55L mutant Fyn SH3 domain. A transient folding intermediate is detected for both of the proteins studied here, and the dispersion data are well fit to a folding model of the form F ↔ I ↔ U, where F, I, and U correspond to folded, intermediate, and unfolded states, respectively. The temperature dependencies of the folding/unfolding rate constants were obtained so that the thermodynamic properties of each of F, I, and U could be established. The detection of I states in folding pathways of all SH3 domains examined to date via relaxation dispersion NMR spectroscopy indicates that such intermediates may well be a conserved feature in the folding of such domains in general but that their transient nature along with their low population makes detection difficult using more well-established approaches to the study of folding.

An understanding of how an unfolded polypeptide chain achieves its native conformation can only be obtained through characterization of the intermediate and transition states that participate in the folding reaction, as well as elucidation of how the properties of these states depend on amino acid composition and on the native state tertiary fold. A number of recent experimental and computational studies of protein folding have focused on addressing whether proteins belonging to the same family and/or sharing a similar tertiary structure fold through the same pathway (*1*−*3*). These studies primarily involved comparison of folding transition states (as determined by $\phi$-value analysis (*4*, *5*)) of families of small proteins that exhibit reversible two-state folding behavior (*3*). Some protein families such as SH3 domains (*6*, *7*) and Ig-like domains (*8*, *9*) were shown to fold via similar pathways, however other proteins such as Suc1 and Cks1 that have a high sequence similarity and share the same $\alpha/\beta$ fold possess very different transition state structures (*10*).

Src homology 3 (SH3) domains are small (∼60 residue) protein modules that fold into five-stranded $\beta$-sandwiches comprised of two orthogonal $\beta$-sheets. These modules are found in a number of multidomain proteins, primarily those involved in cellular signaling (*11*). The folding behavior of a number of SH3 domains has been characterized in detail by protein engineering methods and found to be consistent with a two-state process according to calorimetric, equilibrium, and kinetic folding/refolding experiments (*7*, *12*−*18*). These studies have provided a detailed picture of a highly polarized transition state that is conserved within SH3 domains, in which a portion of the central $\beta$-sheet including strands $\beta$2, $\beta$3, and $\beta$4 is formed, while N- and C-terminal $\beta$-strands ($\beta$1 and $\beta$5) and the RT-src loop remain largely unstructured.

Recent NMR studies of two mutational variants of the Fyn SH3 domain, where the highly conserved residue Gly48 is replaced by either Val or Met, have provided a more detailed picture for SH3 domain folding that involves formation of a low populated on-pathway intermediate (*19*−*21*). In these studies, relaxation dispersion NMR experiments have been used that are very sensitive to micro- to millisecond ($\mu$s−

† This work was supported by a grant from the Canadian Institutes of Health Research (CIHR) to L.E.K. P.N. and D.M.K. acknowledge postdoctoral support from the Deutsche Forschungsgemeinschaft (NE 1197/1-1) and the CIHR, respectively. L.E.K. holds a Canada Research Chair in Biochemistry.

* Corresponding author. Phone: (416) 978-0741. Fax: (416) 978-6885. E-mail: kay@pound.med.utoronto.ca.

‡ Department of Biochemistry.

§ Department of Chemistry.

# Department of Medical Genetics.

10.1021/bi0611560 CCC: $33.50 
Published on Web 08/03/2006

ms) time-scale exchange processes linking the ground state to multiple excited confirmations (*22*). $^{1}H$, $^{15}N$, and $^{13}C$ experiments of this sort (*23*−*28*) have been performed to study the millisecond time-scale folding of G48V and G48M Fyn SH3 domains using nearly all backbone amide and side-chain methyl groups of Ile, Leu, and Val residues as probes of the folding process. A transient folding intermediate (I) populated at the level of 1−2% in exchange with the folded (F) and unfolded (U) states has been observed for both mutants examined. Structural models of the folding intermediate of the Fyn SH3 domain based on the extracted $^{15}N$ chemical shift differences between F, I, and U states (*19*) are remarkably similar to the folding transition state that emerges from $\phi$-value analysis (*7*, *14*, *17*). Relaxation dispersion measurements have been performed as a function of temperature (*19*) and pressure (*29*) and on samples with varying levels of protein deuteration (*21*) to characterize the thermodynamic and volumetric properties of F, I, and U states, providing insight into the changes in both chain hydration and packing along the folding pathway of the Fyn SH3 domain.

To date, only the G48V and G48M mutants of the Fyn SH3 domain have been studied by NMR relaxation dispersion methods (*19*−*21*), and the generality of the F ↔ I ↔ U folding model for SH3 domain folding is open to question. For example, (i) is the presence of a detected intermediate simply an "artifact" of mutations at position 48 or (ii) perhaps a reflection of some special sequence properties that are unique to the Fyn SH3 domain, or (iii) are such intermediates common to SH3 domain folding in general but not detected by less sensitive techniques? To address these questions, we studied an additional pair of SH3 domains, including a A39V/N53P/V55L mutant of the SH3 domain from the Fyn tyrosine kinase (referred to in what follows as A39V/N53P/V55L Fyn SH3) where the conserved Gly (G48) is retained and a G48V mutant of an otherwise stabilized SH3 domain from Abp1p (G48V Abp1p SH3; see Materials and Methods) (*30*), a 592-residue protein that plays important roles in regulating the actin cytoskeleton in yeast (*31*, *32*). Notably, G48V Abp1p SH3 has only 36% sequence identity to the Fyn SH3 domain. Relaxation dispersion experiments indicate conclusively that these two proteins also fold through an on-pathway intermediate state, I. In addition, we present here an analysis of the structure of the I state for G48V Abp1p SH3 showing that it is very similar to the I states that have been characterized for G48M and G48V Fyn SH3 (*19*), as well as the "one-dimensional energy landscape" of the G48V Abp1p folding reaction derived from the temperature dependence of the folding/unfolding kinetics. The results from the present study suggest that formation of the I state observed originally in studies of G48V and G48M Fyn SH3 may be a general feature of SH3 domain folding.

## MATERIALS AND METHODS

Samples of the $^{15}N$-labeled G48V mutant of a hyperstable Abp1p SH3 domain from *Saccharomyces cerevisiae* (the hyperstable protein is generated from WT with E7L, V21K, and N23G mutations) and the A39V/N53P/V55L mutant of the Fyn SH3 domain were expressed in *Escherichia coli* as amino- and carboxyl-terminal hexa-histidine fusions, respectively, and purified as described previously (*33*). The N-terminal tag associated with the Abp1p G48V SH3 domain was cleaved using TEV protease, while the C-terminal tag on the Fyn module was retained in this study. Samples were 1.0 mM in protein, 50 mM sodium phosphate, 0.05% $NaN_3$, 0.2 mM EDTA, pH 7, 10% $D_2O$. Backbone $^{1}H$ and $^{15}N$ resonance assignments for both proteins were obtained from [$^{1}H$, $^{15}N$]-NOESY-HSQC and [$^{1}H$, $^{15}N$]-TOCSY-HSQC experiments (*34*).

$^{15}N$ single-quantum Carr-Purcell-Meiboom-Gill (CPMG) dispersion profiles for G48V Abp1p SH3 (A39V/N53P/V55L Fyn SH3) were recorded at field strengths of 11.7 and 18.8 T at temperatures of 40, 43, and 46 °C (35, 40, and 45 °C) using the pulse scheme of Tollinger et al. (*28*). Relaxation dispersion profiles were generated from peak intensities, $I_1(\nu_{CPMG})$, measured in a series of 17 2D $^{1}H$-$^{15}N$ correlation maps employing 14 values of the CPMG field strength, $\nu_{CPMG}$, ranging from 50 (41.7 for A39V/N53P/V55L Fyn SH3) to 1000 Hz, with a constant-time relaxation delay, $T_{relax}$, of 40 (48) ms, and with a pair of duplicate points recorded for error analysis. Peak intensities were extracted using the MUNIN approach (*35*, *36*) and were converted into effective relaxation rates $R_{2,eff} = -1/T_{relax}\ln(I_1(\nu_{CPMG})/I_0)$, where $I_0$ is the peak intensity in the reference spectrum obtained with $T_{relax} = 0$ (*37*). Uncertainties in $R_{2,eff}$ values were estimated as described previously (*20*). In cases where calculated errors of $R_{2,eff}$ were less than 2% (1.5%), a minimum value of 2% (1.5%) was used.

Relaxation dispersion data for $n_r = 37$ (45) residues of G48V Abp1p SH3 (A39V/N53P/V55L Fyn SH3) that have non-overlapped cross-peaks in $^{1}H-^{15}N$ correlation spectra and with exchange contributions $R_{ex} = R_{2,eff}(50\ Hz) - R_{2,eff}(1000\ Hz) > 2.5\ s^{-1}$, measured at $n_t = 3$ temperatures and $n_f = 2$ magnetic fields (a total of $n_{dat} = 3108$ (3780) data points) were fit together to models of two-, F ↔ U, and three-, F ↔ I ↔ U, site exchange as described in detail elsewhere (*19*, *20*). Briefly, fits were performed by adjusting exchange parameters, described below, to minimize a function of the form $\chi^2 = \sum(R_{2,eff}^{observed} - R_{2,eff}^{calculated})^2/\sigma_{R_{2,eff}}^2$, where $\sigma_{R_{2,eff}}$ is the experimental uncertainty of each $R_{2,eff}$ value and the sum extends over all measurements included in the fit. $R_{2,eff}^{calculated}$ values were obtained from numerical integration of the Bloch−McConnell equations (*38*) using in-house written software. The data were analyzed under the assumptions that (i) the chemical shift differences between the exchanging states $\Delta\varpi_{ij} = \varpi_i - \varpi_j$, are independent of temperature, (ii) the folding process at each site can be described with the same exchange rate constants, with the temperature dependence of the rate constant for the transition from state $i$ to state $j$ ($i,j \in \{F, I, U\}$) given by transition-state theory

$$k_{i\rightarrow j} = (k_B\kappa T/h)\exp(-\Delta G^{\ddagger}_{ij}/(RT)) \qquad (1)$$

and (iii) the intrinsic relaxation rates are the same for a given probe in states F, I, and U (simulations have established that this is a valid approximation for the exchange parameters here). In eq 1, $\Delta G^{\ddagger}_{ij} = \Delta H^{\ddagger}_{ij} - T\Delta S^{\ddagger}_{ij}$ is the activation free energy for the process of conversion from state $i$ to $j$, $\Delta S^{\ddagger}_{ij}$ and $\Delta H^{\ddagger}_{ij}$ are the activation entropy and enthalpy, respectively, $k_B$, $h$, and $R$ are Boltzman's, Plank's, and the universal gas constants, and $\kappa$ is a transmission coefficient. A value of $\kappa = 1.6 \times 10^{-7}$ was used as an empirical estimate for protein folding reactions (*39*), corresponding to $k_B\kappa/h = 3000$

$s^{-1}$ $K^{-1}$, but thermodynamic parameters obtained with $\kappa = 1$ are reported as well. The model of two-site exchange, F ↔ U, for G48V Abp1p SH3 (A39V/N53P/V55L Fyn SH3) includes $n_{par} = n_t n_f n_r + n_r + 4 = 263$ (319) adjustable parameters ($n_t n_f n_r$ values of intrinsic relaxation rates that are assumed to be the same for F and U states along with $n_r$ values of $\Delta\varpi_{FU}$ and the four activation parameters $\Delta H^{\ddagger}_{FU}$, $\Delta S^{\ddagger}_{FU}$, $\Delta H^{\ddagger}_{UF}$, and $\Delta S^{\ddagger}_{UF}$). There are $n_{dat} - n_{par} = 2845$ (3461) degrees of freedom. The three-site exchange model, F ↔ I ↔ U, includes $n_{par} = n_t n_f n_r + 2n_r + 8 = 304$ (368) adjustable parameters ($n_t n_f n_r$ values of intrinsic relaxation rates assumed to be the same for the F, I, and U states, $2n_r$ values of $\Delta\varpi_{FI}$ and $\Delta\varpi_{FU}$, and the eight activation parameters $\Delta H^{\ddagger}_{FI}$, $\Delta S^{\ddagger}_{FI}$, $\Delta H^{\ddagger}_{IF}$, $\Delta S^{\ddagger}_{IF}$, $\Delta H^{\ddagger}_{IU}$, $\Delta S^{\ddagger}_{IU}$, $\Delta H^{\ddagger}_{UI}$, and $\Delta S^{\ddagger}_{UI}$) corresponding to 2804 (3412) degrees of freedom. Extensive minimizations with different initial conditions were performed using the optimization protocol described previously for G48V and G48M Fyn SH3 that involves both grid searches and optimizations based on a Levenberg−Marquardt algorithm (*40*), to ensure that the minimum energy solution is found (*19*, *20*). Uncertainties in the extracted model parameters were estimated using the covariance matrix method (*40*). Errors in $\Delta\varpi_{FI}$ and $\Delta\varpi_{FU}$ values for G48V Abp1p SH3 were obtained by a bootstrap procedure (*41*) in which some fraction of the 3108 experimental $R_{2,eff}$ values was removed from the original data set. In this approach, each of the 3108 experimental $R_{2,eff}$ values was numbered consecutively, 3108 random numbers were generated from 1 to 3108, and an experimental data point was retained for analysis if its designated number was in the set of 3108 random numbers chosen. Note that in this approach some data points can be selected multiple times, while others are not chosen. The resulting dispersions were subsequently refit starting from the best fit solution to the complete data set. The process was repeated 50 times, and the errors in $\Delta\varpi$ were calculated as one standard deviation of the distribution of values obtained.

## RESULTS AND DISCUSSION

*NMR Methodology*. In this work, we used $^{15}$N relaxation dispersion NMR methods to study the folding reactions of a pair of SH3 domains, referred to in what follows as G48V Abp1p SH3 and A39V/N53P/V55L Fyn SH3. The goal is to extend our original studies of the G48M and G48V Fyn SH3 domains, showing that the folding of both of these mutants proceeds through an intermediate on-pathway state (*19*−*21*) with structural properties similar to those elucidated for the transition state of the assumed two-state folding reaction (*7*, *14*, *17*).

$^{15}$N CPMG relaxation dispersion experiments are extremely sensitive to millisecond time-scale exchange processes between ground and excited state conformations, so long as the later are populated at a level of approximately 0.5% or higher and there are distinct chemical shifts between the exchanging conformers (*22*). The experiments are particularly powerful because there is no requirement that correlations from excited states be visible in NMR spectra (indeed they are usually not, as in the present case). Along with the kinetics (exchange rate constants) and the thermodynamics (populations of exchanging states) of the process, the technique also can provide structural information about minor conformations in the form of $^{15}$N chemical shifts (*22*, *42*). As protein folding is accompanied by large chemical shift changes (generally between 1 and 10 ppm for backbone $^{15}$N), relaxation dispersion methods have emerged as an ideal tool for studying folding/unfolding equilibria in marginally stable proteins/destabilized mutants with unfolding free energies, $\Delta G_{UF}$, of 1−3 kcal/mol and folding rates on the millisecond time-scale (*19*, *43*, *44*). The stability of the wild-type Fyn SH3 domain is well outside this range (4.4 kcal/mol, 25 °C) (*45*), and although $\Delta G_{UF}$ for the wild-type Abp1p SH3 module is 3.1 kcal/mol (25 °C) (*30*), the folding/unfolding rates for this domain are too slow to give rise to quantifiable dispersions. As a result, we have studied mutational variants of these modules that satisfy the stability and folding rate requirements indicated above over the temperature range investigated (35−46 °C), resulting in high-quality $^{15}$N CPMG dispersion profiles for the majority of the backbone $^{15}$N probes (see below). In the case of the Fyn SH3 domain, mutation of A39 and V55 to V and L, respectively, increases both folding and unfolding rates by an order of magnitude, while substitution of P for N at position 53 decreases $\Delta G_{UF}$ to 2.6 kcal/mol (40 °C), so that the folding kinetics and thermodynamics are optimal for detection by the CPMG dispersion class of experiment. To increase the folding rate of the Abp1p SH3 module, three substitutions were made, E7L, V21K, and N23G, that elevate the folding rate by 10-fold and also stabilize the protein, followed by the G48V mutation that increases the rate of folding still further, yet decreases $\Delta G_{UF}$ to within the range indicated above (*30*).

*Two-Site vs Three-Site Exchange Models*. The folding reaction of G48V Abp1p SH3 and A39V/N53P/V55L Fyn SH3 have been analyzed using $^{15}$N CPMG dispersion profiles measured at two static magnetic field strengths and three temperatures for 37 (Abp1p SH3) and 45 (Fyn SH3) amide groups that show considerable exchange contributions to the $^{15}$N transverse relaxation rates (see Materials and Methods). Initially, relaxation dispersion data are fit on a per-residue basis to a two-site exchange model, F ↔ U, to extract unfolding, $k_{F\rightarrow U}$, and folding, $k_{U\rightarrow F}$ rates as reported by each amide $^{15}$N probe. Since a folding/unfolding process described by the model, F ↔ U, is a cooperative global event involving all residues in the protein, all backbone amides should report the same folding and unfolding rates (to within uncertainties). If different rates are, in fact, observed experimentally then this is strong evidence that the two-state model is not appropriate.

Figure 1 shows distributions of folding, $k_{U\rightarrow F}$, and unfolding, $k_{F\rightarrow U}$, rates for selected residues of stabilized G48V Abp1p SH3 (panel a) and A39V/N53P/V55L Fyn SH3 (panel b). Here parameters have been estimated via a jackknife procedure (*40*) in which 25% of the data from each dispersion profile was removed and the resultant curves were fit to obtain exchange parameters. This process was repeated 25 times to generate a distribution (i.e., 25 sets) of parameters that provides a measure of the range of ($k_{U\rightarrow F}$, $k_{F\rightarrow U}$) values that are consistent with the experimental data. It is clear that for G48V Abp1p SH3 $k_{U\rightarrow F}$ values can differ by as much as an order of magnitude (for data recorded at 40 °C), while $k_{F\rightarrow U}$ rates vary severalfold, with variations in the rates far exceeding those predicted on the basis of the error bounds. Differences in per-residue values of folding and unfolding rates for A39V/N53P/V55L Fyn SH3 are even greater,

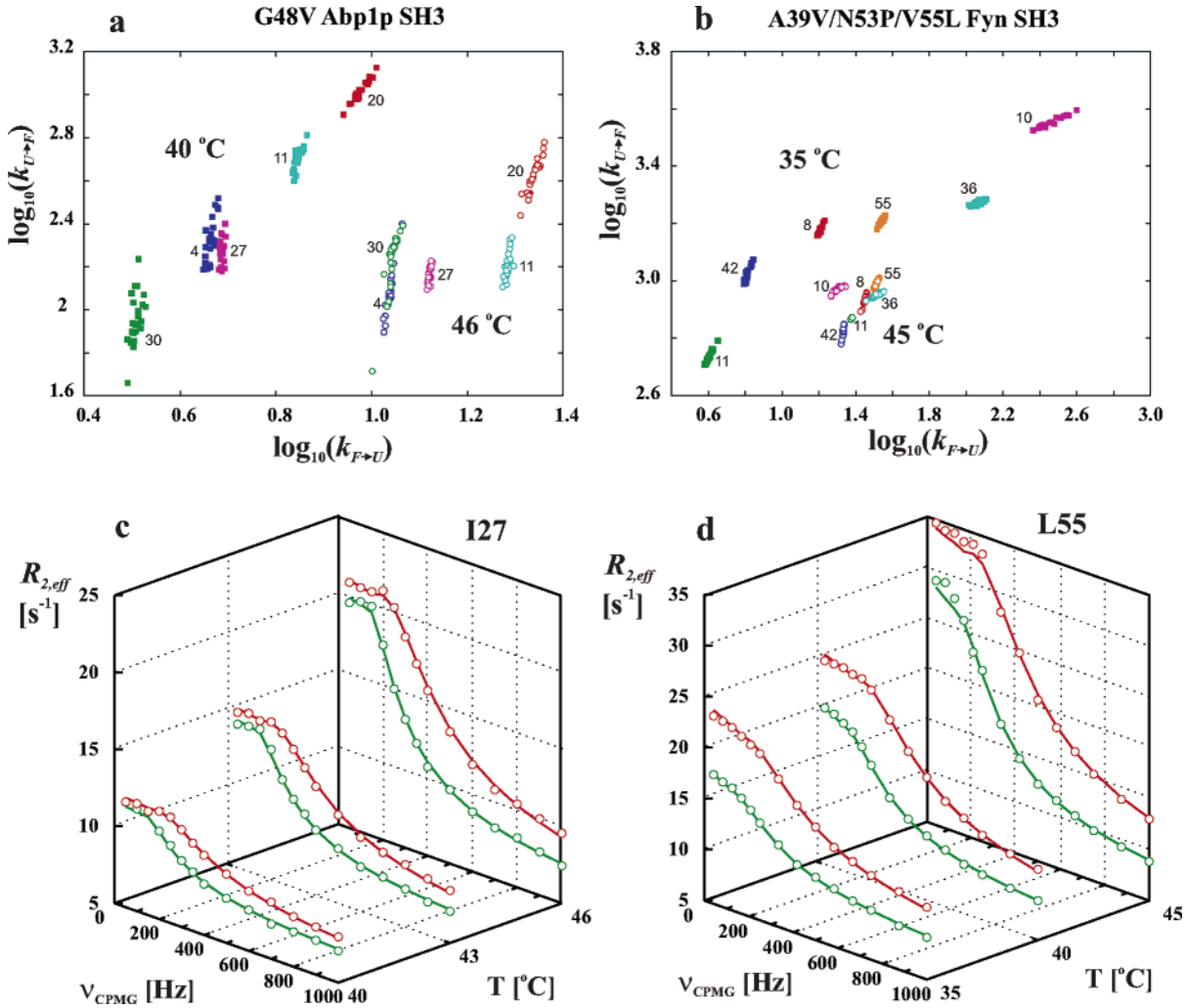


FIGURE 1: Distributions of folding, $k_{U\rightarrow F}$, and unfolding, $k_{F\rightarrow U}$, rates obtained on a per-residue basis from an analysis of $^{15}$N CPMG dispersion profiles for selected residues (labeled with residue numbers) of (a) stabilized G48V Abp1p SH3 at 40 °C (filled boxes) and 46 °C (open circles) and (b) A39V/N53P/V55L Fyn SH3 at 35 °C (filled boxes) and 45 °C (open circles). Dispersion curves for each residue were analyzed independently, as described in the text, and distributions of parameters obtained via a jackknife procedure (*40*) described previously (*43*) and in the text; rate constant distributions for a given residue are shown with the same color. For each residue, data measured at two magnetic fields and three temperatures were fit together using a model of two-site exchange F ↔ U along with the assumptions that (i) the $^{15}$N chemical shift differences $\Delta\varpi_{FU}$ are independent of temperature and that (ii) the temperature dependence of the rate constants is given by transition state theory (eq 1). (c,d) Typical fits of dispersion data using a global three-site exchange model (solid lines) for residues (c) Ile27 of G48V Abp1p SH3 and (d) Leu55 of A39V/N53P/V55L Fyn SH3. Although the fits are shown for only select residues, data from all residues, all temperatures, and all magnetic fields were included in the analysis. Dispersion profiles (circles) in red and green were recorded at spectrometer fields of 18.8 and 11.7 T, respectively.

approaching 1 and 2 orders of magnitude for $k_{U\rightarrow F}$ and $k_{F\rightarrow U}$, respectively, at 35 °C. These results indicate that $^{15}$N CPMG dispersion data for both SH3 domains are not consistent with a two-state folding/unfolding process.

Additional evidence for a more complex folding pathway for both G48V Abp1p SH3 and A39V/N53P/V55L Fyn SH3 is also provided from a statistical analysis of global fits of $^{15}$N dispersion data using two-site and three-site exchange models (Table 1). Here a single set of exchange parameters was used to fit all of the $^{15}$N dispersion data simultaneously (profiles measured at two magnetic fields and three temperatures; see Materials and Methods) for all of the residues showing dispersions in each of the proteins (approximately 40). In the case of data from G48V Abp1p SH3 and A39V/N53P/V55L Fyn SH3 poor fits were obtained to the two-site exchange model F ↔ U; reduced $\chi^2$ values (i.e., ratios of the $\chi^2$ target function to the number of degrees of freedom of the model) of 2.4 and 6.5 were obtained (probability of accepting the model $P(\chi^2)$ is close to 0). In contrast, the global three-site exchange model, F ↔ I ↔ U, was able to reproduce the data well with reduced $\chi^2$ values of 1.06 and 0.92 for the Abp1p and Fyn SH3 domains, respectively. $\chi^2$ values are very sensitive to estimates of experimental errors. Therefore, the quality of data fitting also has been established

Table 1: $\chi^2$ Target Functions Obtained In Global Fits of $^{15}$N Single-Quantum CPMG Dispersion Profiles for 37 (45) Residues of Abp1 SH3 (Fyn SH3) Mutants Measured at Three Temperatures and Two Magnetic Fields Using Two- and Three-Site Exchange Models[a]

| | G48V (E7L/V21K/N23G) Abp1 SH3 | | A39V/N53P/V55L Fyn SH3 | |
|---|---|---|---|---|
| model | $\chi^2$ | no. degrees of freedom | $\chi^2$ | no. degrees of freedom |
| two-site | 6913 | 2845 | 22456 | 3461 |
| three-site | 2975 | 2804 | 3131 | 3412 |

[a] See Materials and Methods for details of data fits.

Table 2: Folding Kinetics Parameters Obtained in Global Fits of $^{15}$N Single-Quantum CPMG Dispersion Data for 37 (45) Residues of Abp1p SH3 (Fyn SH3) Mutants Using Two- and Three-Site Exchange Models[a]

| G48V (E7L/V21K/N23G) Abp1 SH3 | | | | | | |
|---|---|---|---|---|---|---|
| | two-site model | | three-site model | | | |
| temp [°C] | $k_{F\to U} + k_{U\to F}$ [s$^{-1}$] | $p_U$ [%] | $k_{F\to I} + k_{I\to F}$ [s$^{-1}$] | $k_{I\to U} + k_{U\to I}$ [s$^{-1}$] | $p_I$ [%] | $p_U$ [%] |
| 40 | 360 ± 15 | 1.42 ± 0.06 | 1460 ± 112 | 1797 ± 101 | 0.67 ± 0.04 | 1.55 ± 0.07 |
| 43 | 348 ± 6 | 2.45 ± 0.06 | 1488 ± 96 | 2012 ± 98 | 1.05 ± 0.04 | 2.62 ± 0.08 |
| 46 | 339 ± 2 | 4.15 ± 0.02 | 1520 ± 101 | 2252 ± 111 | 1.61 ± 0.07 | 4.34 ± 0.12 |
| A39V/N53P/V55L Fyn SH3 | | | | | | |
| | two-site model | | three-site model | | | |
| temp [°C] | $k_{F\to U} + k_{U\to F}$ [s$^{-1}$] | $p_U$ [%] | $k_{F\to I} + k_{I\to F}$ [s$^{-1}$] | $k_{I\to U} + k_{U\to I}$ [s$^{-1}$] | $p_I$ [%] | $p_U$ [%] |
| 35 | 940 ± 25 | 0.89 ± 0.01 | 2656 ± 47 | 1428 ± 27 | 1.64 ± 0.03 | 0.65 ± 0.01 |
| 40 | 892 ± 14 | 1.63 ± 0.02 | 4396 ± 110 | 1912 ± 41 | 1.53 ± 0.03 | 1.39 ± 0.01 |
| 45 | 853 ± 13 | 2.91 ± 0.03 | 7162 ± 294 | 2975 ± 130 | 1.43 ± 0.05 | 2.88 ± 0.02 |

[a] See Materials and Methods for details of data fits.

by F-test analyses (*40*), showing that the three-site model provides a statistically significant improvement in fit relative to that obtained via the two-site model, with the global $\chi^2$ value decreased by 2.3(7.2) fold, i.e., by 3938 (19325), with only 41 (49) additional adjustable parameters added for G48V Abp1p SH3 (A39V/N53P/V55L Fyn SH3). It is important to emphasize that the three-site exchange model that was used in all fits of the data makes no assumption as to whether I is on-pathway. That is, a model of the form F ↔ A ↔ B was employed, where A,B ∈{I, U}. As described above, among the parameters extracted from fits of the relaxation dispersion data are chemical shift differences between exchanging states, $\Delta\varpi$, that can be extremely useful in defining the nature of the process that is studied. For both systems considered here the lowest energy solutions are those for which the chemical shifts of state B correspond very closely to random-coil values as predicted by the CSI module of the program NMRView (*46*, *47*), confirming that the exchange process studied is one that derives from a folding/unfolding reaction and consistent with an on-pathway folding intermediate, I.

Examples of fits of $^{15}$N CPMG dispersion data to the global three-site exchange model are provided in Figure 1c (Ile 27 of G48V Abp1p SH3) and 1d (Leu55 of A39V/N53P/V55L Fyn SH3), showing that the relaxation profiles can be well fit to the F ↔ I ↔ U model. In principle, more complex folding models than the linear three-site scheme can be employed, and statistical criteria used to establish whether improvements in the fits justify the increased number of fitting parameters. However, the F ↔ I ↔ U model considered here fits the data to within error (Table 1), and we do not feel that further insight into the folding mechanism would be derived through more complex analyses.

*Global Two-Site and Three-Site Exchange Parameters*. Table 2 shows populations of the exchanging states and rates of interconversion between states for G48V Abp1p SH3 and A39V/N53P/V55L Fyn SH3 obtained from fits to the three-site exchange model. For completeness, the parameters generated from the two-site fits are also indicated. For G48V Abp1p SH3, the population of the I state, $p_I$, is less than that of the U state, $p_U$, at all temperatures considered. In contrast, for A39V/N53P/V55L Fyn SH3, $p_U < p_I$ at temperatures lower than 40 °C and for temperatures of approximately 25 °C or lower, the population of the U state decreases to the point where dispersion profiles obtained for this system can be well fit to a global two-site exchange model corresponding to F ↔ I (data not shown). Below we focus on the G48V Abp1p SH3 domain and a comparison of the folding parameters for this protein with those obtained from our previous studies of G48V and G48M Fyn SH3 (*19*); a detailed analysis of the folding of A39V/N53P/V55L Fyn SH3 will be presented elsewhere.

*Structural Properties of the Folding Intermediate of G48V Abp1p SH3*. Backbone $^{15}$N chemical shifts are a sensitive function of the electronic environment surrounding the nitrogen nuclei and can be used as qualitative reporters of local backbone conformation (*19*). Therefore, $^{15}$N chemical shift differences, $\Delta\varpi_{FI}$ ($\varpi_F - \varpi_I$) and $\Delta\varpi_{FU}$ ($\varpi_F - \varpi_U$), obtained from an analysis of $^{15}$N CPMG relaxation dispersion data using the three-site exchange model contain structural information about the conformational ensemble of the folding intermediate I. Previously, we have derived structural models for the I states of G48V and G48M Fyn SH3 based on the ratio $\Delta = \Delta\varpi_{FI}/\Delta\varpi_{FU}$ measured at each backbone amide site for which dispersion data was available (*19*). A value of $\Delta = 0$ indicates that the $^{15}$N chemical shift at a particular backbone site in the folding intermediate I coincides with that of the folded state F, suggesting similar backbone conformations for the I and F states at this site. By contrast, $\Delta = 1$ indicates that $^{15}$N chemical shifts for a particular site in states I and U coincide, consistent with an "unfolded-like" intermediate state at this position.

Figure 2 shows $\Delta = \Delta\varpi_{FI}/\Delta\varpi_{FU}$ ratios for G48V Abp1p SH3 plotted as a function of residue number (panel a) and color-coded on the structure of the wild-type protein (panel b; spheres correspond to the backbone amide nitrogens). For comparison, Δ values for G48V Fyn SH3 that are available from a previous study (*19*) are coded on its structure (panel c). The Δ ratios for G48V Abp1p SH3 point to a reasonably well organized intermediate state I, with formation of nativelike secondary structure in most regions with the exception of the extended RT-src loop. For example, $|\Delta|$ values below 0.3 are observed for most backbone amide groups, with the exception of Glu7−Val21 of the RT-src loop and residues Leu49 and Val55 that are spatially close to the loop in the folded state. Residues of the RT-src loop have Δ ratios higher than 0.3−0.4, with Δ very close to 1.0 for Asp11, Glu14, Asp15, and Phe20. Locally "structured"

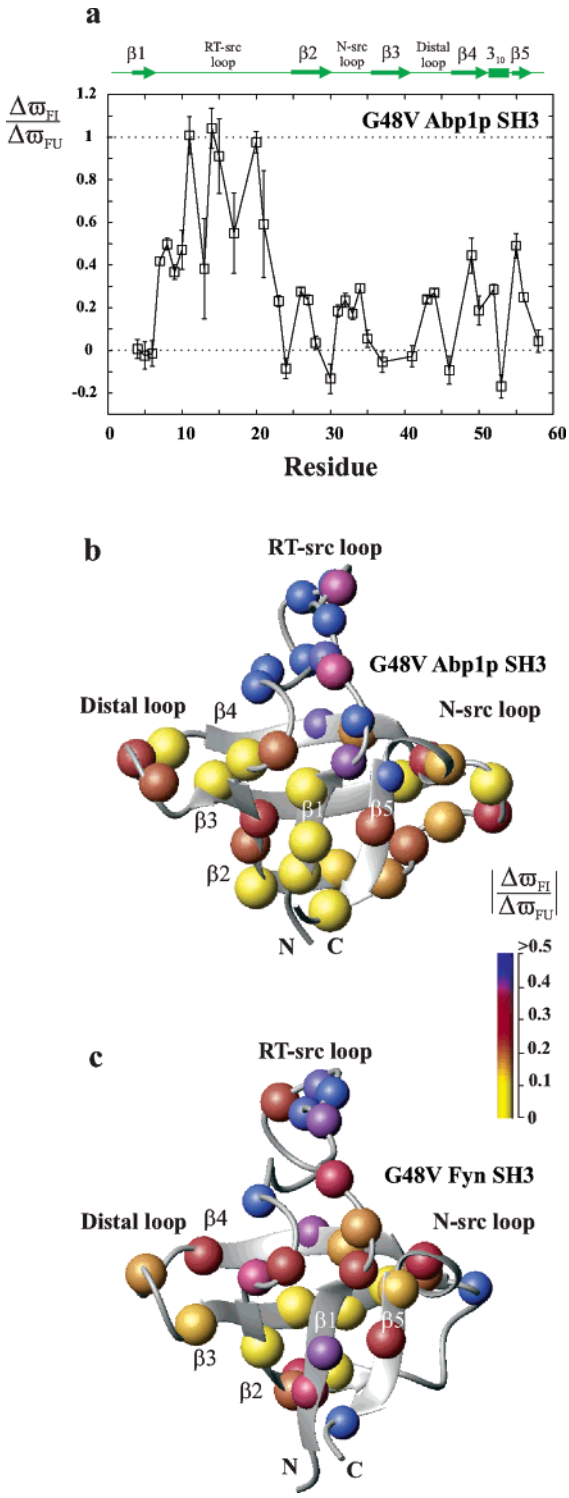


FIGURE 2: Ratio of $^{15}$N chemical shift differences $\Delta = \Delta\varpi_{FI}/\Delta\varpi_{FU}$ for G48V Abp1p SH3 (a) plotted as a function of residue number (errors indicated by vertical lines) and (b) color coded on the structure of the wild-type protein (*53*) (PDB identifier 1JO8), where each sphere in the diagram is a backbone amide nitrogen position. The secondary structure of the Apb1p SH3 domain is included in (a). (c) Values of $\Delta$ obtained in a previous $^{15}$N CPMG dispersion study of the G48V Fyn SH3 domain (*19*) color coded on the structure of the wild-type protein (*54*) (PDB identifier 1SHF). Only residues with $|\Delta\varpi_{FU}| > 1.5$ ppm are included.

backbone regions of the I state ensemble of G48V Abp1p SH3 are similar to those identified in our previous studies of G48V and G48M Fyn SH3 (compare, for example, $|\Delta|$ ratios for G48V mutants of Abp1p and Fyn SH3 domains in Figure 2, panels b and c, respectively), with $\beta$-strands $\beta2-\beta4$ at least partially formed in the I state. It is notable, however, that residues corresponding to the N- and C-terminal $\beta$-strands ($\beta1$ and $\beta5$) in the folded domain are in a more nativelike conformation in the I state of G48V Abp1p than in I states of either G48V or G48M Fyn SH3. It may well be that the I state of G48V Abp1p SH3 corresponds to a later stage intermediate than either of the intermediate states that have been observed in dispersion studies of G48V or G48M Fyn SH3. In this context, repeating the dispersion analysis described above and elsewhere (*19*−*21*) on a series of mutants provides an opportunity to obtain snapshots of structure formation along the folding trajectory. As a final point, it is worth noting again that regions of nativelike contacts observed in the I states of both G48V Abp1p and Fyn SH3 (Figure 2b,c) from dispersion studies are similar to what has been seen from $\phi$-value analysis (*7*, *14*, *17*), providing additional evidence that the I states observed in the NMR work are on-pathway.

*Thermodynamic Parameters along the Folding Pathway of G48V Abp1p SH3.* By recording $^{15}$N CPMG relaxation dispersion profiles as a function of temperature, it is possible to extract the enthalpic, $\Delta H$, and entropic, $T\Delta S$, contributions to the free energy changes, $\Delta G$ between states F, I, and U along the three-site folding trajectory. Moreover, the temperature dependence of the exchange rates can be used to obtain the activation parameters $\Delta H^{\ddagger}_{ij}$, $\Delta S^{\ddagger}_{ij}$, and $\Delta G^{\ddagger}_{ij}$ ($i,j \in$ {F, I, U}), as described in detail previously (*19*, *43*). However, their interpretation must be made with caution because unlike $\Delta G$, $\Delta H$, and $\Delta S$ that do not depend on the transmission coefficient, $\kappa$, in eq 1 (see Materials and Methods), $\Delta S^{\ddagger}_{ij}$ and $\Delta G^{\ddagger}_{ij}$ do (*43*). Figure 3a shows $G$, $H$, and $TS$ profiles for the folding reaction of the Abp1p SH3 domain that have been obtained from the temperature study reported here (at 43 °C). For comparison, similar profiles for G48V Fyn SH3 (at 17.5 °C) obtained in a previous study (*19*) are provided in Figure 3b. Curves with solid lines are generated using $\kappa = 1.6 \times 10^{-7}$, a value obtained based on an empirical estimate for protein folding (*39*), whereas profiles shown with dashed lines correspond to $\kappa = 1$. It has been assumed that $\Delta S^{\ddagger}_{ij}$, $\Delta H^{\ddagger}_{ij}$ (and $\Delta S_{ij}$, $\Delta H_{ij}$) are independent of temperature over the small temperature range examined in both studies (40−46 °C and 10−25 °C for Abp1p and Fyn SH3 domains, respectively). The thermodynamic and activation parameters for the folding of G48V Abp1p and G48V Fyn SH3 domains derived from the F ↔ I ↔ U model and their associated errors are listed in tabular form in Supporting Information.

Not surprisingly, the relatively small free energy difference between the folded and unfolded states of G48V Abp1p SH3 (G48V Fyn SH3), $\Delta G_{FU} = G_F - G_U = -2.3$ (−1.8) kcal/mol, is the result of large, mutually compensating enthalpic and entropic terms, $\Delta H_{FU} = -35.3$ (−6.7) kcal/mol and $T\Delta S_{FU} = -33.0$ (−4.9) kcal/mol. Interestingly, $\Delta H_{UF}$ and $T\Delta S_{UF}$ values measured for G48V Abp1p SH3 at 43 °C are significantly larger than those obtained for G48V Fyn SH3 at 17.5 °C (*19*) (see Figure 3). We have also noted a similar relationship between $\Delta H_{UF}$ and $T\Delta S_{UF}$ values obtained for the folding reactions of F61A/A90G and F61A/I72A mutants of a redesigned apocytochrome $b_{562}$ protein that were studied over temperature ranges of 37.5−47.5 and 17.5−32.5 °C, respectively; namely, much larger values are obtained for

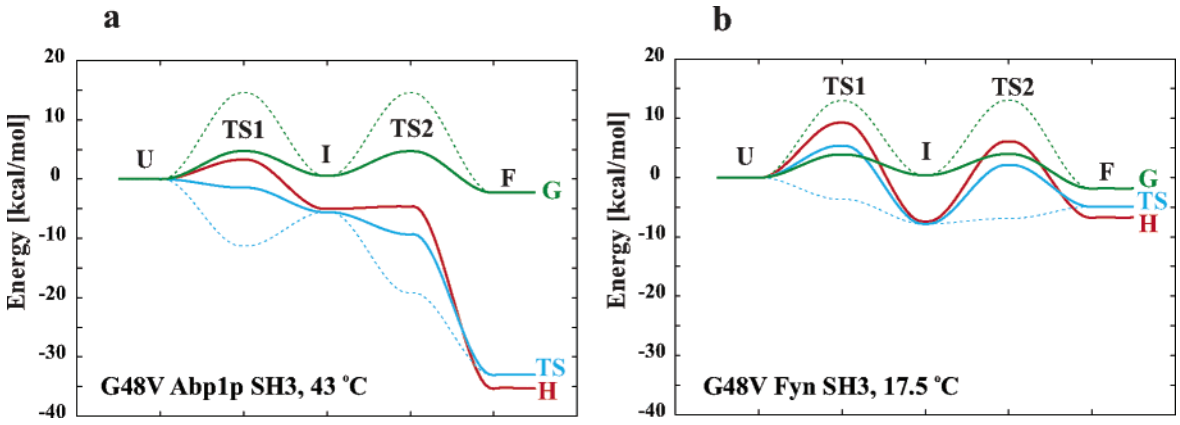


FIGURE 3: Profiles of free energy, $\Delta G$ (green), in addition to the enthalpic $\Delta H$ (red) and entropic $T\Delta S$ (blue) contributions to $\Delta G$ along the folding pathway of (a) G48V Abp1p SH3 at 43 °C and (b) G48V Fyn SH3 at 17.5 °C (*19*). $\Delta G$ and $T\Delta S$ profiles shown with solid lines are generated using the transmission coefficient $\kappa = 1.6 \times 10^{-7}$, while profiles shown with dashed lines are obtained with $\kappa = 1$ (eq 1). The U state is taken as the reference.

the protein studied at elevated temperature (*43*). Differences in thermodynamics parameters between the pairs of SH3 domains in Figure 3 or between the apocyctochrome mutants studied previously no doubt reflect changes in primary structure between each of the domains (recall that 64% of the residues in Abp1p and Fyn SH3 domains are different). However, the differences also reflect the delicate balance between contributions to enthalpy and entropy of folding from both the protein and the solvent and the changes in the relative importance of each of the contributions with temperature. Focusing first on entropy, there is a significant penalty associated with protein compaction and with rigidification of side-chain positions, and this penalty is expected to increase with temperature because the entropy of the unfolded state ensemble increases more rapidly with temperature than that of the folded state (*48*, *49*). On the other hand, release of water that accompanies folding results in an increase in the entropy of the system that favors the folding process. This effect becomes less favorable, however, with increasing temperature because hydration water that surrounds exposed hydrophobic groups in the U state becomes less well ordered (*4*, *50*). Thus, the entropy difference between "bound" and free water is less pronounced at higher temperatures. The net effect (i.e., sum of contributions from protein and solvent) produces the large change in $\Delta S_{UF}$ observed for Abp1p SH3 (experiments recorded at the higher temperature) and the comparatively smaller difference noted for Fyn SH3 at the lower temperature. In a similar manner, the decrease in ordering of waters of hydration in the U state and the concomitant higher enthalpy of hydration that accompanies an increase in temperature (i.e., nonpolar hydration is opposed by enthalpy at higher temperatures) contributes to the more negative change in enthalpy of folding that is observed in the comparison between the two SH3 domains of Figure 3. Of course, the solvent effects described above are captured in the large and negative heat capacity change that accompanies protein folding (*4*) that leads to $\Delta H_{FU}$ ($H_F - H_U$) and $\Delta S_{FU}$ becoming more negative with temperature.

Molecular dynamics simulations of protein folding of SH3 domains (*51*, *52*), as well as volumetric studies of Fyn SH3 domain folding from our laboratory (*29*), suggest that a significant fraction of water release upon folding in this class of molecule occurs between states I and F along the folding trajectory. This result and the discussion presented above provide a rationale for the large differences in observed values of $\Delta H_{IF}$ and $\Delta S_{IF}$ between the Abp1p and Fyn SH3 domains quantified at temperatures of 43 and 17.5 °C, respectively. Note that while the amide $^{15}$N chemical shifts of the I states in the folding pathways for both of these proteins are consistent with the formation of significant nativelike backbone structure, it is most likely that the side-chain conformations are highly disordered, as has been observed in a recent study involving $^{13}$C relaxation dispersion spectroscopy of the Ile, Leu, and Val methyl groups in G48M Fyn SH3 (*21*). Thus, a large fraction of the "ordering" that accompanies the I to F transition for both proteins and that contributes to the differences in their $\Delta H_{IF}$ and $\Delta S_{IF}$ values very likely derives from the side-chains.

Although activation free energies $\Delta G^{\ddagger}_{ij}$, enthalpies $\Delta H^{\ddagger}_{ij}$, and entropies $\Delta S^{\ddagger}_{ij}$, ($i,j \in \{F, I, U\}$) can in principle be extracted from the temperature dependence of the folding rates, $k_{i\rightarrow j}$, we prefer not to analyze these values in detail because they depend on the model used to interpret the temperature−rate dependence in the first place (eq 1) and for $\Delta S^{\ddagger}_{ij}$, $\Delta G^{\ddagger}_{ij}$ on the choice of $\kappa$. Nevertheless, even a very conservative analysis suggests that the folding barrier from I to F in the G48V Abp1p SH3 domain (Figure 3a) is entropic, since this result is obtained over the range $\kappa \leq 1$ and is in keeping with the picture that emerges from the interpretation of $\Delta H_{IF}$ and $\Delta S_{IF}$ for Abp1p SH3 given above.

## CONCLUDING REMARKS

We have presented results of $^{15}$N relaxation dispersion studies of protein folding for a pair of SH3 domains, including the G48V mutant of a stabilized SH3 module from Abp1p and the A39V/N53P/V55L mutant of an SH3 domain from Fyn. The data are not consistent with a two-state model of protein folding, F ↔ U, but are well explained by a three-state model, F ↔ I ↔ U, where the transient intermediate state is populated at a level of 1−2%, depending on the temperature. The presence of an intermediate state in the folding pathway of a pair of SH3 domains, G48M and G48V mutants of Fyn SH3, has been observed previously in dispersion studies (*19*−*21*); the results presented here based on studies of two additional SH3 modules establish that (i) the I state detected previously is not an "artifact" of mutations

at the highly conserved G48 position (ii) nor a specific feature that is unique to the primary sequence of the Fyn SH3 domain but rather very likely a general feature of SH3 domain folding and (iii) that the folding of different SH3 domains likely proceeds through similar pathways, as has been suggested previously (*6*, *7*). From the temperature dependence of the folding kinetics of G48V Abp1p SH3 a "one-dimensional" energy landscape of the folding reaction of the protein was obtained. The thermodynamics data and the $^{15}$N chemical shift differences between the F, I, and U states support a model of an intermediate state that is significantly hydrated and that contains "nativelike" backbone structure, with the exception of the RT-src loop that is largely unfolded. Although the details of the I folding intermediate of A39V/N53P/V55L Fyn SH3 will be presented elsewhere, it is noteworthy that this intermediate shares many of the same structural features with those observed for G48M and G48V Fyn and G48V Abp1p SH3 domains, including formation of the central $\beta$-sheet. Finally, it is worth restating that previous experimental studies of the folding of SH3 domains that are based on the addition of denaturant and/or that make use of only a very small number of probes of folding are consistent with a two-state mechanism (*7*, *12*−*18*). The present work along with previous NMR dispersion studies from our laboratory (*19*−*21*) establishes that the folding reaction is more complex and that by using many probes (in this case, $^{15}$N backbone amide sites for nearly every position in the protein) it is possible to obtain much more detailed information than is available from other more 'traditional' methodologies that have been used to study protein folding in the past.

## SUPPORTING INFORMATION AVAILABLE

Table S1 listing the thermodynamic and activation parameters for the folding of G48V Abp1p and G48V Fyn SH3 domains derived from the F ↔ I ↔ U model. This material is available free of charge via the Internet at http://pubs.acs.org.

## REFERENCES


1. Baker, D. (2000) A surprising simplicity to protein folding, *Nature 405*, 39−42.
2. Gunasekaran, K., Eyles, S. J., Hagler, A. T., and Gierasch, L. M. (2001) Keeping it in the family: folding studies of related proteins, *Curr. Opin. Struct. Biol. 11*, 83−93.
3. Zarrine-Afsar, A., Larson, S. M., and Davidson, A. R. (2005) The family feud: do proteins with similar structures fold via the same pathway? *Curr. Opin. Struct. Biol. 15*, 42−49.
4. Fersht, A. (1999) *Structure and Mechanism in Protein Science: A Guide to Enzyme Catalysis and Protein Folding*, W. H. Freeman, New York.
5. Matouschek, A., Kellis, J. T., Serrano, L., and Fersht, A. R. (1989) Mapping the transition-state and pathway of protein folding by protein engineering, *Nature 340*, 122−126.
6. Capaldi, A. P., and Radford, S. E. (1998) Kinetic studies of beta-sheet protein folding, *Curr. Opin. Struct. Biol. 8*, 86−92.
7. Martinez, J. C., and Serrano, L. (1999) The folding transition state between SH3 domains is conformationally restricted and evolutionarily conserved, *Nat. Struct. Biol. 6*, 1010−1016.
8. Geierhaas, C. D., Paci, E., Vendruscolo, M., and Clarke, J. (2004) Comparison of the transition states for folding of two Ig-like proteins from different superfamilies, *J. Mol. Biol. 343*, 1111−1123.
9. Hamill, S. J., Cota, E., Chothia, C., and Clarke, J. (2000) Conservation of folding and stability within a protein family: The tyrosine corner as an evolutionary cul-de-sac, *J. Mol. Biol. 295*, 641−649.
10. Seeliger, M. A., Breward, S. E., and Itzhaki, L. S. (2003) Weak cooperativity in the core causes a switch in folding mechanism between two proteins of the cks family, *J. Mol. Biol. 325*, 189−199.
11. Pawson, T., and Gish, G. D. (1992) SH2 and SH3 domains − from structure to function, *Cell 71*, 359−362.
12. Filimonov, V. V., Azuaga, A. I., Viguera, A. R., Serrano, L., and Mateo, P. L. (1999) A thermodynamic analysis of a family of small globular proteins: SH3 domains, *Biophys. Chem. 77*, 195−208.
13. Grantcharova, V. P., and Baker, D. (1997) Folding dynamics of the src SH3 domain, *Biochemistry 36*, 15685−15692.
14. Northey, J. G. B., Di Nardo, A. A., and Davidson, A. R. (2002) Hydrophobic core packing in the SH3 domain folding transition state, *Nat. Struct. Biol. 9*, 126−130.
15. Northey, J. G. B., Maxwell, K. L., and Davidson, A. R. (2002) Protein folding kinetics beyond the Phi value: Using multiple amino acid substitutions to investigate the structure of the SH3 domain folding transition state, *J. Mol. Biol. 320*, 389−402.
16. Plaxco, K. W., Guijarro, J. I., Morton, C. J., Pitkeathly, M., Campbell, I. D., and Dobson, C. M. (1998) The folding kinetics and thermodynamics of the Fyn-SH3 domain, *Biochemistry 37*, 2529−2537.
17. Riddle, D. S., Grantcharova, V. P., Santiago, J. V., Alm, E., Ruczinski, I., and Baker, D. (1999) Experiment and theory highlight role of native state topology in SH3 folding, *Nat. Struct. Biol. 6*, 1016−1024.
18. Viguera, A. R., Martinez, J. C., Filimonov, V. V., Mateo, P. L., and Serrano, L. (1994) Thermodynamic and kinetic-analysis of the Sh3 domain of spectrin shows a 2-state folding transition, *Biochemistry 33*, 2142−2150.
19. Korzhnev, D. M., Salvatella, X., Vendruscolo, M., Di Nardo, A. A., Davidson, A. R., Dobson, C. M., and Kay, L. E. (2004) Low-populated folding intermediates of Fyn SH3 characterized by relaxation dispersion NMR, *Nature 430*, 586−590.
20. Korzhnev, D. M., Neudecker, P., Mittermaier, A., Orekhov, V. Y., and Kay, L. E. (2005) Multiple-site exchange in proteins studied with a suite of six NMR relaxation dispersion experiments: An application to the folding of a Fyn SH3 domain mutant, *J. Am. Chem. Soc. 127*, 15602−15611.
21. Mittermaier, A., Korzhnev, D. M., and Kay, L. E. (2005) Side-chain interactions in the folding pathway of a Fyn SH3 domain mutant studied by relaxation dispersion NMR spectroscopy, *Biochemistry 44*, 15430−15436.
22. Palmer, A. G. (2004) NMR characterization of the dynamics of biomacromolecules, *Chem. Rev. 104*, 3623−3640.
23. Ishima, R., and Torchia, D. A. (2003) Extending the range of amide proton relaxation dispersion experiments in proteins using a constant-time relaxation-compensated CPMG approach, *J. Biomol. NMR 25*, 243−248.
24. Korzhnev, D. M., Kloiber, K., Kanelis, V., Tugarinov, V., and Kay, L. E. (2004) Probing slow dynamics in high molecular weight proteins by methyl-TROSY NMR spectroscopy: Application to a 723-residue enzyme, *J. Am. Chem. Soc. 126*, 3964−3973.
25. Korzhnev, D. M., Kloiber, K., and Kay, L. E. (2004) Multiple-quantum relaxation dispersion NMR spectroscopy probing millisecond time-scale dynamics in proteins: Theory and application, *J. Am. Chem. Soc. 126*, 7320−7329.
26. Orekhov, V. Y., Korzhnev, D. M., and Kay, L. E. (2004) Double- and zero-quantum NMR relaxation dispersion experiments sampling millisecond time scale dynamics in proteins, *J. Am. Chem. Soc. 126*, 1886−1891.
27. Skrynnikov, N. R., Mulder, F. A. A., Hon, B., Dahlquist, F. W., and Kay, L. E. (2001) Probing slow time scale dynamics at methyl-containing side chains in proteins by relaxation dispersion NMR measurements: Application to methionine residues in a cavity mutant of T4 lysozyme, *J. Am. Chem. Soc. 123*, 4556−4566.
28. Tollinger, M., Skrynnikov, N. R., Mulder, F. A. A., Forman-Kay, J. D., and Kay, L. E. (2001) Slow dynamics in folded and unfolded states of an SH3 domain, *J. Am. Chem. Soc. 123*, 11341−11352.
29. Bezsonova, I., Korzhnev, D. M., Prosser, R. S., Forman-Kay, J. D., and Kay, L. E. (2006) Hydration and packing along the folding pathway of SH3 domains by pressure-dependent NMR, *Biochemistry 45*, 4711−4719.
30. Rath, A., and Davidson, A. R. (2000) The design of a hyperstable mutant of the Abp1p SH3 domain by sequence alignment analysis, *Protein Sci. 9*, 2457−2469.
31. Lila, T., and Drubin, D. G. (1997) Evidence for physical and functional interactions among two *Saccharomyces cerevisiae* SH3

domain proteins, an adenylyl cyclase-associated protein and the actin cytoskeleton, *Mol. Biol. Cell 8*, 367−385.
32. Drubin, D. G., Mulholland, J., Zhu, Z. M., and Botstein, D. (1990) Homology of a yeast actin-binding protein to signal transduction proteins and myosin-I, *Nature 343*, 288−290.
33. Maxwell, K. L., and Davidson, A. R. (1998) Mutagenesis of a buried polar interaction in an SH3 domain: Sequence conservation provides the best prediction of stability effects, *Biochemistry 37*, 16172−16182.
34. Zhang, O. W., Kay, L. E., Olivier, J. P., and Forman-Kay, J. D. (1994) Backbone H-1 and N-15 resonance assignments of the N-terminal Sh3 domain of Drk in folded and unfolded states using enhanced-sensitivity pulsed-field gradient NMR techniques, *J. Biomol. NMR 4*, 845−858.
35. Korzhnev, D. M., Ibraghimov, I. V., Billeter, M., and Orekhov, V. Y. (2001) MUNIN: Application of three-way decomposition to the analysis of heteronuclear NMR relaxation data, *J. Biomol. NMR 21*, 263−268.
36. Orekhov, V. Y., Ibraghimov, I. V., and Billeter, M. (2001) MUNIN: A new approach to multi-dimensional NMR spectra interpretation, *J. Biomol. NMR 20*, 49−60.
37. Mulder, F. A. A., Skrynnikov, N. R., Hon, B., Dahlquist, F. W., and Kay, L. E. (2001) Measurement of slow ($\mu$s-ms) time scale dynamics in protein side chains by N-15 relaxation dispersion NMR spectroscopy: Application to Asn and Gln residues in a cavity mutant of T4 lysozyme, *J. Am. Chem. Soc. 123*, 967−975.
38. McConnell, H. M. (1958) Reaction rates by nuclear magnetic resonance, *J. Chem. Phys. 28*, 430−431.
39. Hagen, S. J., Hofrichter, J., Szabo, A., and Eaton, W. A. (1996) Diffusion-limited contact formation in unfolded cytochrome *c*: Estimating the maximum rate of protein folding, *Proc. Natl. Acad. Sci. U.S.A. 93*, 11615−11617.
40. Press, W. H., Teukolsky, S. A., Vetterling, W. T., and Flannery, B. P. (1997) *Numerical Recipes in C: The Art of Scientific Computing*, 2nd rev. ed., Cambridge University Press, Cambridge.
41. Efron, B., and Tibshirani, R. (1986) Bootstrap methods for standard errors, confidence intervals, and other measures of statistical accuracy, *Stat. Sci.* 54−77.
42. Skrynnikov, N. R., Dahlquist, F. W., and Kay, L. E. (2002) Reconstructing NMR spectra of "invisible" excited protein states using HSQC and HMQC experiments, *J. Am. Chem. Soc. 124*, 12352−12360.
43. Choy, W. Y., Zhou, Z., Bai, Y. W., and Kay, L. E. (2005) An N-15 NMR spin relaxation dispersion study of the folding of a pair of engineered mutants of apocytochrome b(562), *J. Am. Chem. Soc. 127*, 5066−5072.
44. Zeeb, M., and Balbach, J. (2005) NMR spectroscopic characterization of millisecond protein folding by transverse relaxation dispersion measurements, *J. Am. Chem. Soc. 127*, 13207−13212.
45. Di Nardo, A. A., Korzhnev, D. M., Stogios, P. J., Zarrine-Afsar, A., Kay, L. E., and Davidson, A. R. (2004) Dramatic acceleration of protein folding by stabilization of a nonnative backbone conformation, *Proc. Natl. Acad. Sci. U.S.A. 101*, 7954−7959.
46. Johnson, B. A., and Blevins, R. A. (1994) NMR View − a computer-program for the visualization and analysis of NMR data, *J. Biomol.* NMR *4*, 603−614.
47. Schwarzinger, S., Kroon, G. J. A., Foss, T. R., Chung, J., Wright, P. E., and Dyson, H. J. (2001) Sequence-dependent correction of random coil NMR chemical shifts, *J. Am. Chem. Soc. 123*, 2970−2978.
48. Yang, D. W., Mok, Y. K., FormanKay, J. D., Farrow, N. A., and Kay, L. E. (1997) Contributions to protein entropy and heat capacity from bond vector motions measured by NMR spin relaxation, *J. Mol. Biol. 272*, 790−804.
49. Privalov, P. L., and Makhatadze, G. I. (1990) Heat-capacity of proteins. 2. Partial molar heat-capacity of the unfolded polypeptide-chain of proteins − protein unfolding effects, *J. Mol. Biol. 213*, 385−391.
50. Privalov, P. L., and Gill, S. J. (1988) Stability of protein-structure and hydrophobic interaction, *Adv. Protein Chem. 39*, 191−234.
51. Guo, W. H., Lampoudi, S., and Shea, J. E. (2003) Posttransition state desolvation of the hydrophobic core of the src-SH3 protein domain, *Biophys. J. 85*, 61−69.
52. Shea, J. E., Onuchic, J. N., and Brooks, C. L. (2002) Probing the folding free energy landscape of the src-SH3 protein domain, *Proc. Natl. Acad. Sci. U.S.A. 99*, 16064−16068.
53. Fazi, B., Cope, M., Douangamath, A., Ferracuti, S., Schirwitz, K., Zucconi, A., Drubin, D. G., Wilmanns, M., Cesareni, G., and Castagnoli, L. (2002) Unusual binding properties of the SH3 domain of the yeast actin-binding protein Abp1 − Structural and functional analysis, *J. Biol. Chem. 277*, 5290−5298.
54. Noble, M. E. M., Musacchio, A., Saraste, M., Courtneidge, S. A., and Wierenga, R. K. (1993) Crystal-structure of the SH3 domain in human Fyn − comparison of the 3-dimensional structures of SH3 domains in tyrosine kinases and spectrin, *EMBO J. 12*, 2617−2624.

BI0611560